Metabolismo energético

Hábitats y Nichos

Nicho: Espacio abstracto en el ambiente biótico en el cual es posible la vida. Es una combinación única de factores ambientales (bióticos y abióticos) que son capaces de soportar la vida.

Hábitat: Es el componente ambiental o abiótico de un nicho.

Ley de Gause (1934):

a) No existen dos especies ocupando el mismo nicho. Eventualmente, una reemplazará a la otra.

b) Una de las especies evolucionará de modo de ocupar un nicho ligeramente distinto. Generación de una nueva especie.

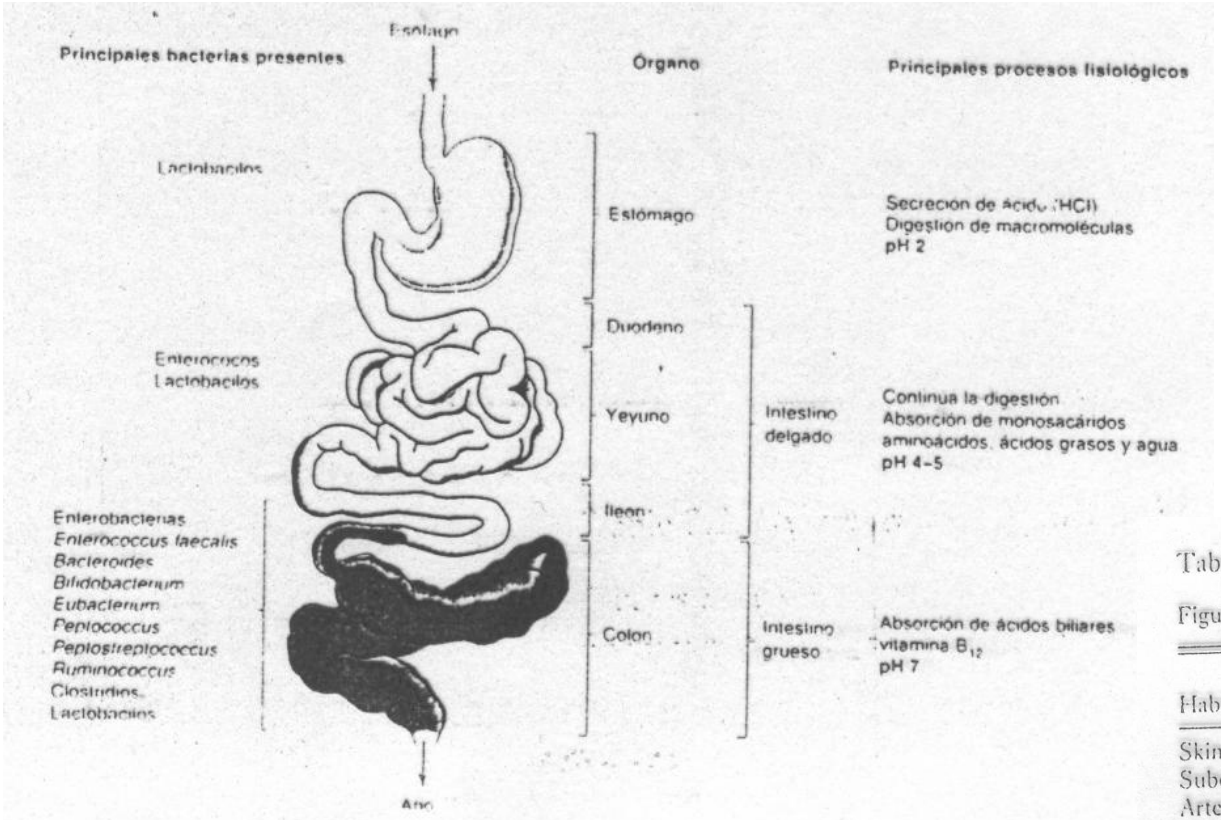

Table 2.2. *Oxygen tensions in some habitats of parasites*

Figures are given i. n mHg.

Habi · ·	Host species	O_2 tension
Skin	man	50–100
Subcutaneous tissue	man, rat, pig	20–43
Arterial blood	man, dog, fish	70–100
Venous blood (heart)	man, horse, duck	37–40
Venous blood (portal vein)	dog, cat	49–66
Peritonea cavity	rabbit, rat, cat	28–40
Pleural cavity	man, monkey	12–39
Urine	man	14–60
Bile	cattle, sheep, dog	0–30
Abomasum (near mucosa)	sheep	4–13
Rumen (gases)	cattle, sheep, goat	0–2
Stomach (gases)	man	0–70
Small intestine (near mucosa)	sheep, rat	4–30
Small intestine (gases)	horse, cattle	0–6
Small intestine (mucosal)	dog	1–57
Small intestine (gases)	pig	8–65
Large intestine (gases)	horse, cattle, rabbit	0–5
Small intestine	duck	0.5–25

Source: Data from von Brand (1952) and Crompton (1979).

SANGRE:
Glucosa: 50-120 mg por 100 ml
Lípidos (160-280 mg/dl FL, 120-125 mg/dl TG, 150-220 mg/dl colesterol)
Aminoácidos, 3-10 mg por 100 ml
Proteínas
pCO2: 40 mm Hg
pH 7.4
Temperatura cte.

Interacciones o Asociaciones:

Comensalismo y foresis

Mutualismo (no obligatorio para existencia)
Simbiosis (obligatorio para existencia)

Parasitismo

Relationships in Nature

BIO108

Interacciones o Asociaciones:

Comensalismo y foresis

Mutualismo (no obligatorio para existencia): *Hydra viridis* (nitrógeno) + *Zoochlorella* (O_2)

Simbiosis (obligatorio para existencia): Termitas (anaerobiosis) + flagelados (nutrientes)
Rumiantes + ciliados

Parasitismo

Interacciones o Asociaciones:

Comensalismo y foresis

Mutualismo (no obligatorio para existencia): *Hydra viridis* (nitrógeno) + *Zoochlorella* (O_2)

Simbiosis (obligatorio para existencia): Termitas (anaerobiosis) + flagelados (nutrientes)
Rumiantes + ciliados

Parasitismo

Parasitismo

Dependencia metabólica

El concepto de dependencia metabólica está estrechamente ligado al de parasitismo. De hecho, puede definirse como parásito a un organismo que, no solo se halla en una continua e íntima asociación con otro (el hospedador), sino que además es metabólicamente dependiente de él.

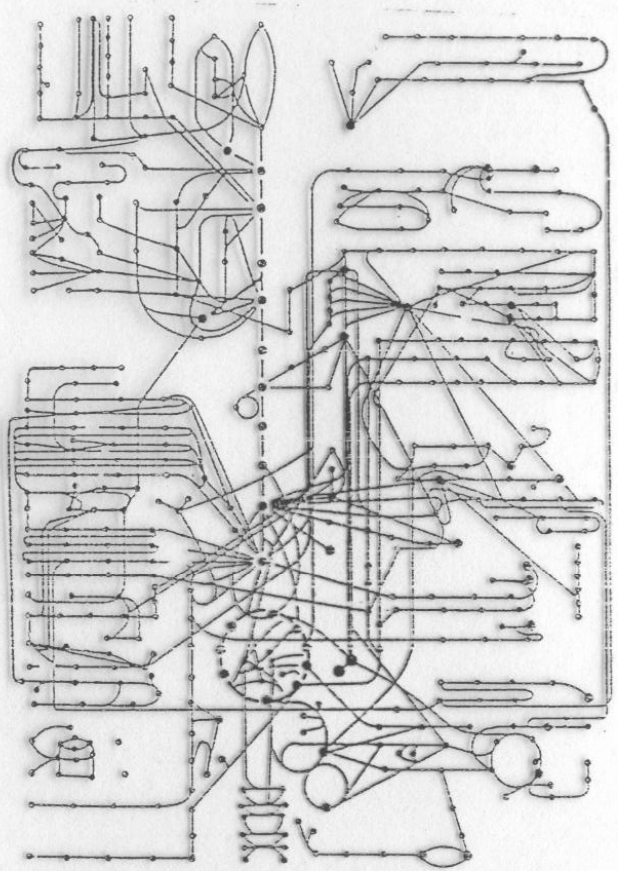

Fig. 1. Major metabolic pathways occurring in mammalian cells. The central importance of the glycolytic pathway and the citric acid cycle is shown in heavy lines. Each dot represents a single metabolite, and enzyme-catalysed reactions are shown by interconnecting lines. No attempt has been made to distinguish anabolic and catabolic processes. Modified from Alberts *et al.* (1983).

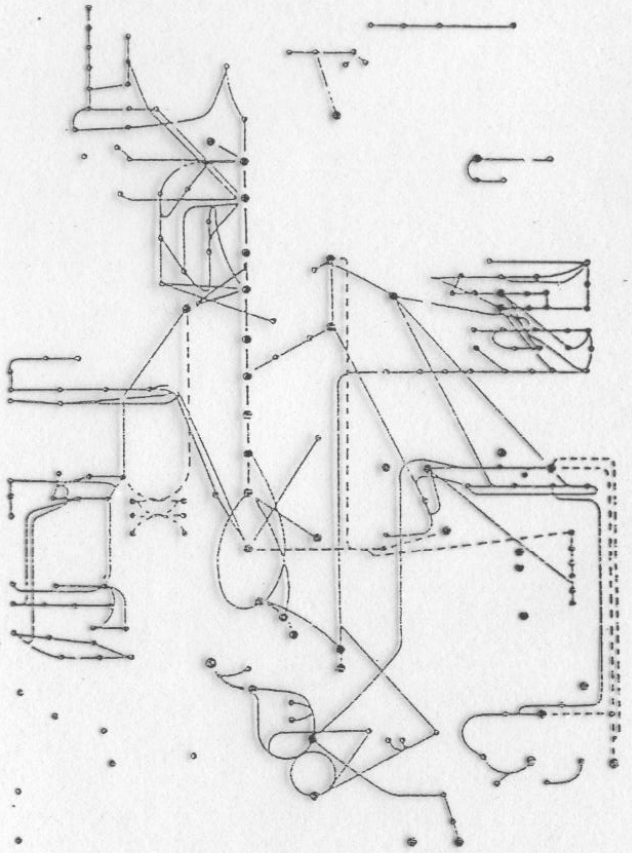

Fig. 2. Major metabolic pathways in the long slender bloodstream trypomastigote form of *Trypanosoma brucei* subspecies. Novel pathways are shown in dotted lines.

Rendimiento energético en parásitos

Producto final	ATP / glucosa
$CO_2 + H_2O$	36
Lactato o etanol	2
Alanina	2
Acetato	2-3
Acetato + Succinato	3.7
Acetato + propionato	5.4
Ac. + Prop. + Acido graso	5

1 nucleus
2 flagellum
3 subpellicular microtubules
4 flagellar pocket
5 endoplasmic reticulum
6 mitochondrion
7 kinetoplast
8 basal body

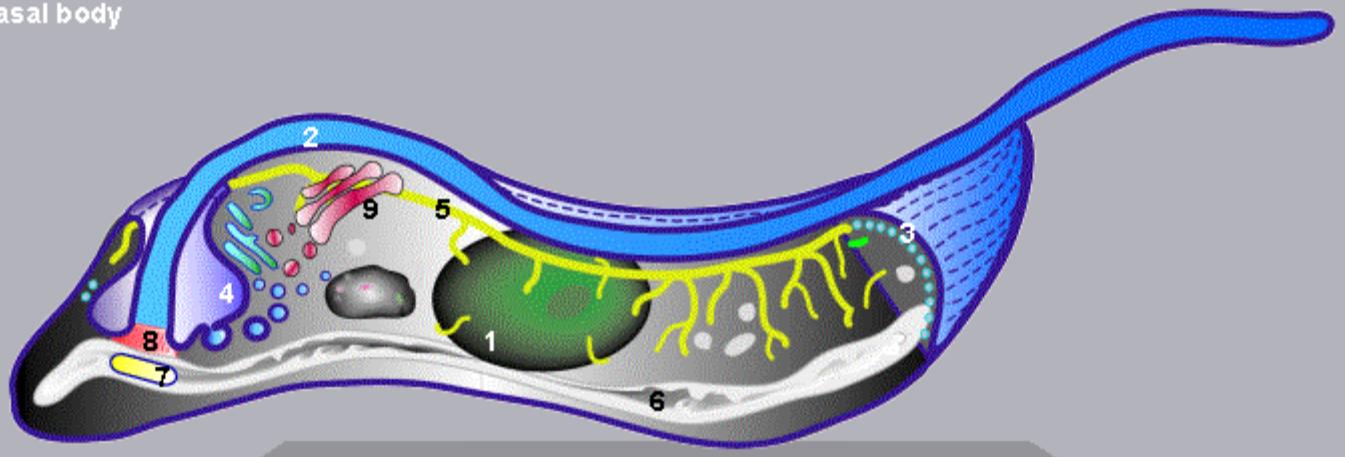

Markus Engstler
Ludwig-Maximilians-Universitaet
Muenchen

INSECTO:
Glucosa: escasa
Lípidos: escasos
Aminoácidos: alta prolina y treoninal
Proteínas
Alta pO_2
Temperatura ambiente

SANGRE:
Glucosa: 50-120 mg por 100 ml
Lípidos (160-280 mg/dl FL, 120-125 mg/dl TG, 150-220 mg/dl colesterol)
Aminoácidos, 3-10 mg por 100 ml
Proteínas
pCO2: 40 mm Hg
pH 7.4
Temperatura cte.

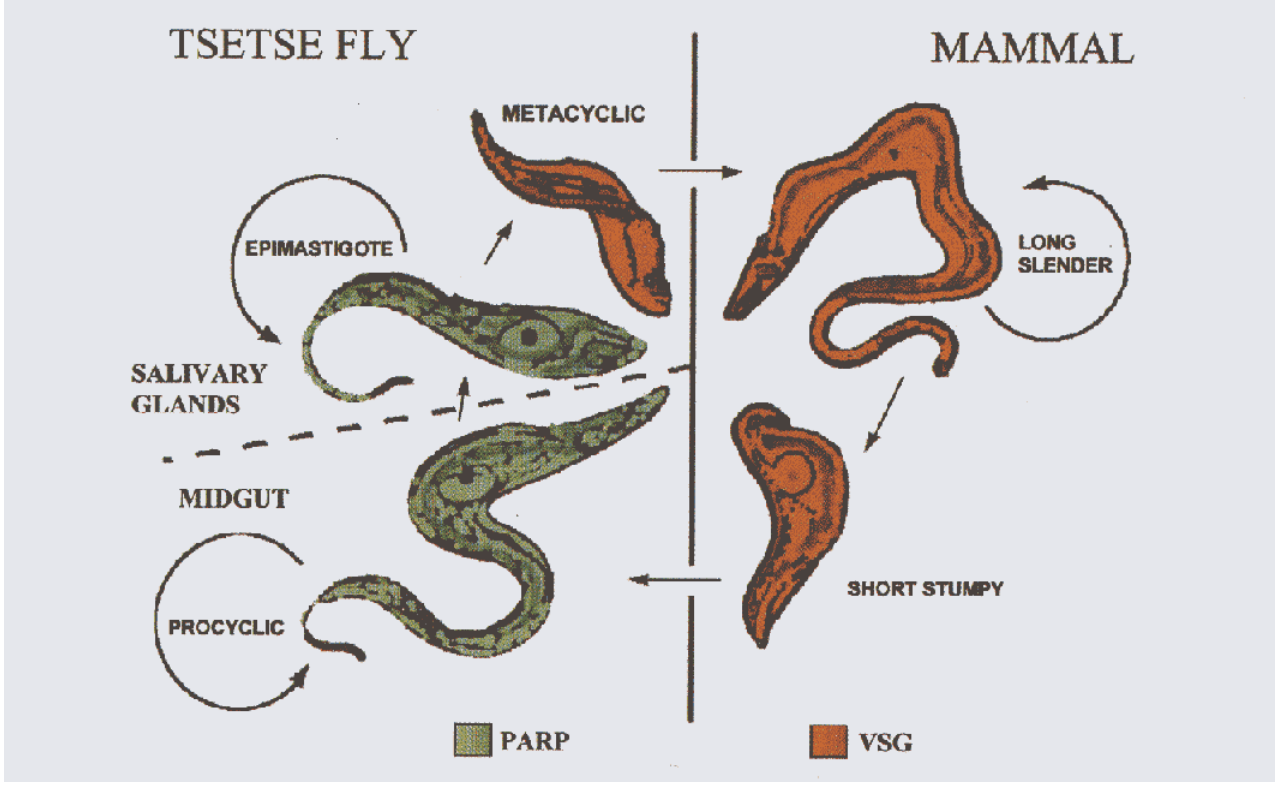

Table 8.1. A. Aerobic glucose consumption by a variety of intact organisms and tissues *in vitro*.

Organism or tissue	Glucose consumption rate (μmol min^{-1} (g wet weight)$^{-1}$)
Saccharomyces cerevisiae	20–30
Pigeon retina	9–15
Ehrlich ascites tumour	11
Trypanosoma brucei, bloodstream form	8
Schistosoma mansoni	1–5
Rat ascites hepatoma	2
Rat skeletal muscle, tetanized	7
at rest	0.03
Guinea pig cerebral cortex	1.4
Rat heart	0.9
Rat liver	0.2
Human erythrocytes	0.05

B. Aerobic glucose consumption by Trypanosomatidae.

Organism	Stage	Glucose consumption rate (μmol min^{-1} (g wet weight)$^{-1}$)
Trypanosoma brucei	Bloodstream form	8.0
	Procyclic form	0.9
Crithidia fasciculata	Choanomastigote	3.8
Leishmania donovani	Promastigote	1.4
L. mexicana	Promastigote	1.3
T. cruzi	Epimastigote	0.7
Phytomonas sp.		5.0

A modified from Shapiro and Talalay (1982) and B from Cazzulo (1992) in which the references to the original data can be found.

TABLE 2.1 Comparison of the glycolytic efficiency of *T. brucei* bloodstream form and glucose-grown yeast

Characteristic	*T. brucei*	Yeast
Glycolytic rate (nmol min^{-1} mg^{-1})	85	50
Glycolytic protein (% of total)	9	60
GAPDH (% of total protein)	0.5	5
Aldolase (% of total protein)	1.2	10
Glycolytic compartment (% of total)	4	> 50
Metabolites involved in the flux (%)	25	100

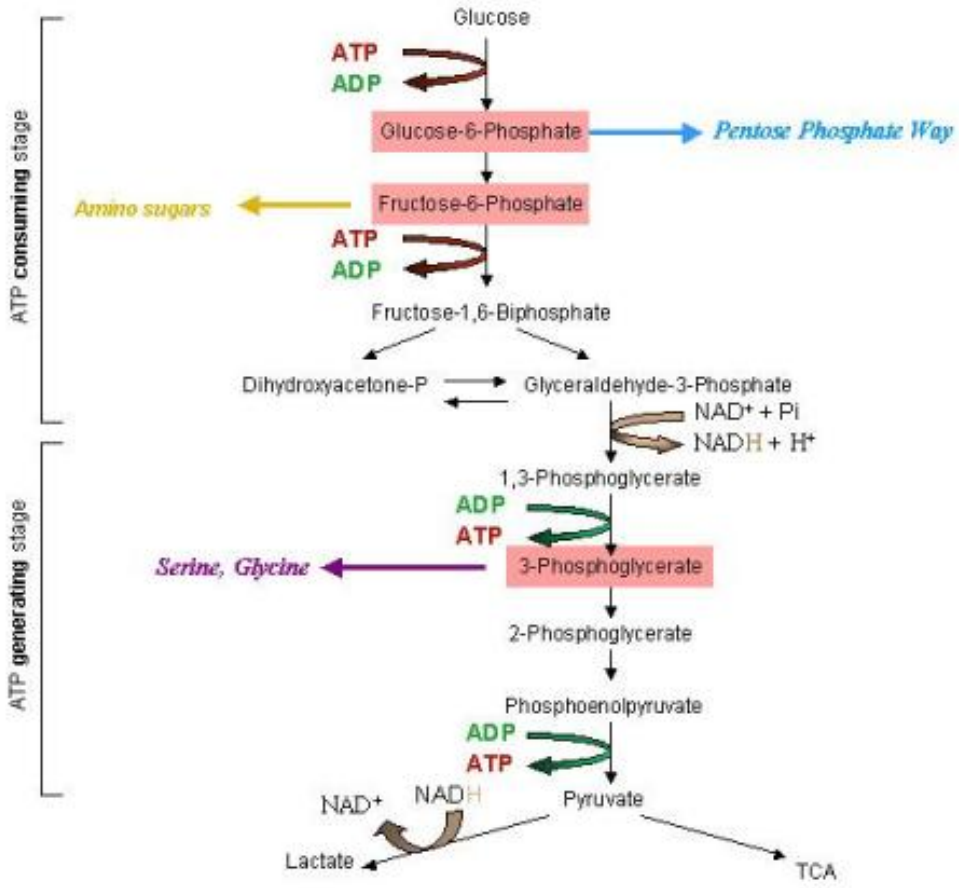
ATP consuming stage
ATP generating stage
Glucose
ATP
ADP
Glucose-6-Phosphate
Pentose Phosphate Way
Amino sugars
Fructose-6-Phosphate
ATP
ADP
Fructose-1,6-Biphosphate
Dihydroxyacetone-P
Glyceraldehyde-3-Phosphate
NAD+ + Pi
NADH + H+
1,3-Phosphoglycerate
ADP
ATP
Serine, Glycine
3-Phosphoglycerate
2-Phosphoglycerate
Phosphoenolpyruvate
ADP
ATP
NAD+
NADH
Pyruvate
Lactate
TCA

Efecto “turbo” en glucólisis

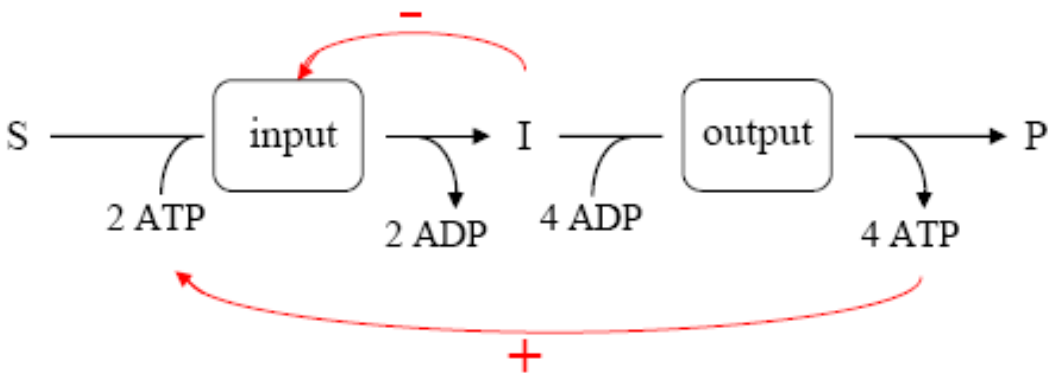

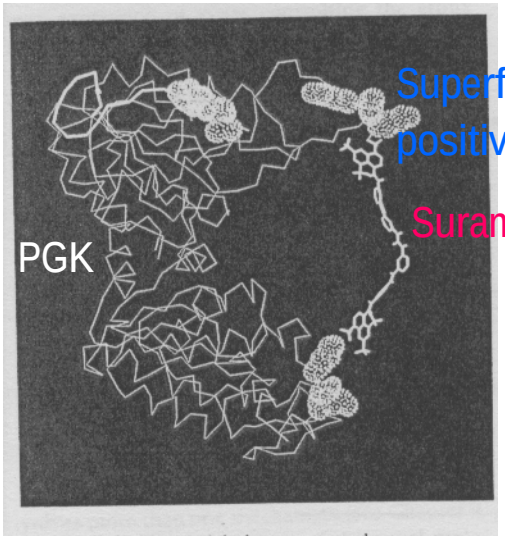

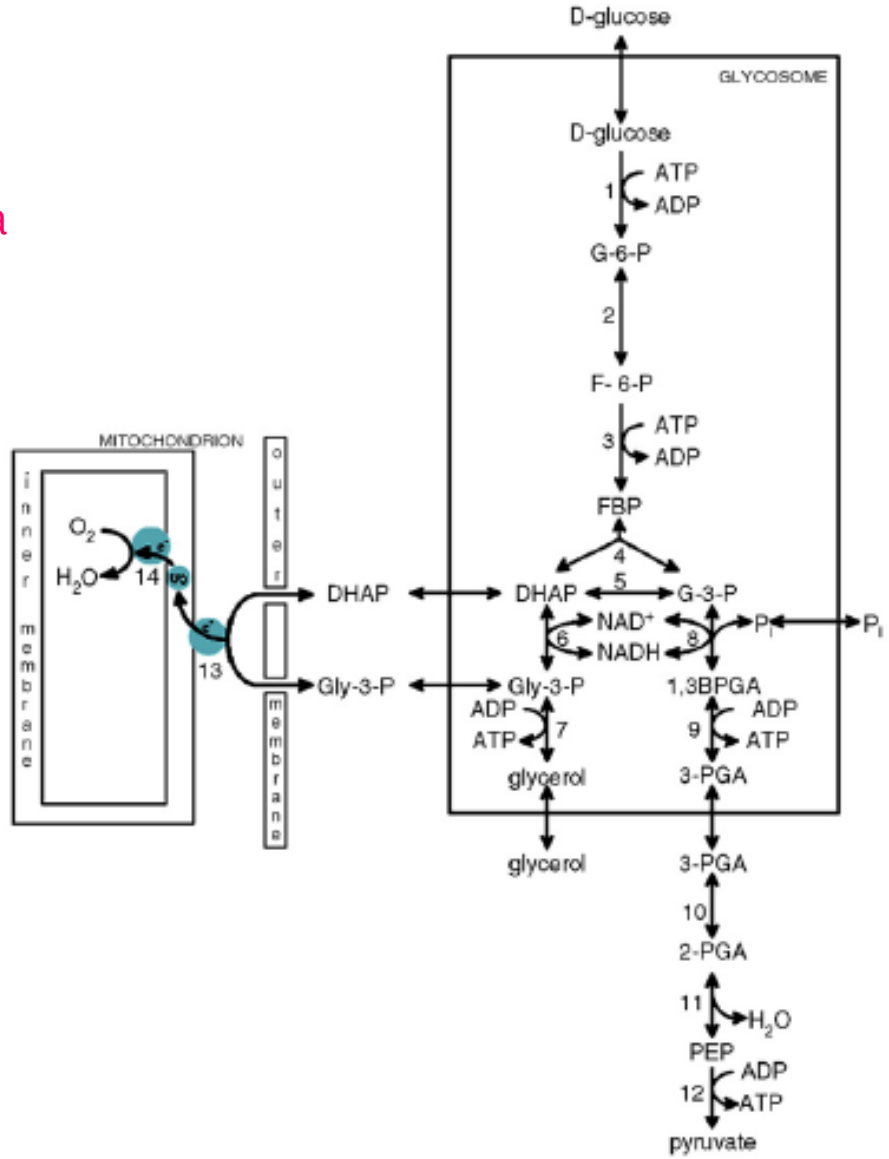

Fig. 1. Schematic representation of glycolysis in the bloodstream-form of *T. brucei*. Under aerobic conditions, glucose is converted into pyruvate. Under anaerobic conditions equimolar amounts of glycerol and pyruvate are produced. Abbreviations: 1,3BPGA, 1,3-bisphosphoglycerate; DHAP, dihydroxyacetone phosphate; F-6-P, fructose 6-phosphate; FBP, fructose 1,6-bisphosphate; G-3-P, glyceraldehyde 3-phosphate; G-6-P, glucose 6-phosphate; Gly-3-P, glycerol 3-phosphate; PEP, phospho*enol*pyruvate; 3-PGA, 3-phosphoglycerate; Pi, inorganic phosphate; UQ, ubiquinone pool. Enzymes are: 1, hexokinase; 2, glucose-6-phosphate isomerase; 3, phosphofructokinase; 4, aldolase; 5, triosephosphate isomerase; 6, glycerol-3-phosphate dehydrogenase; 7, glycerol kinase; 8, glyceraldehyde-3-phosphate dehydrogenase; 9, glycosomal phosphoglycerate kinase; 10, phosphoglycerate mutase; 11, enolase; 12, pyruvate kinase; 13, FAD-dependent glycerol-3-phosphate dehydrogenase; 14, alternative oxidase.

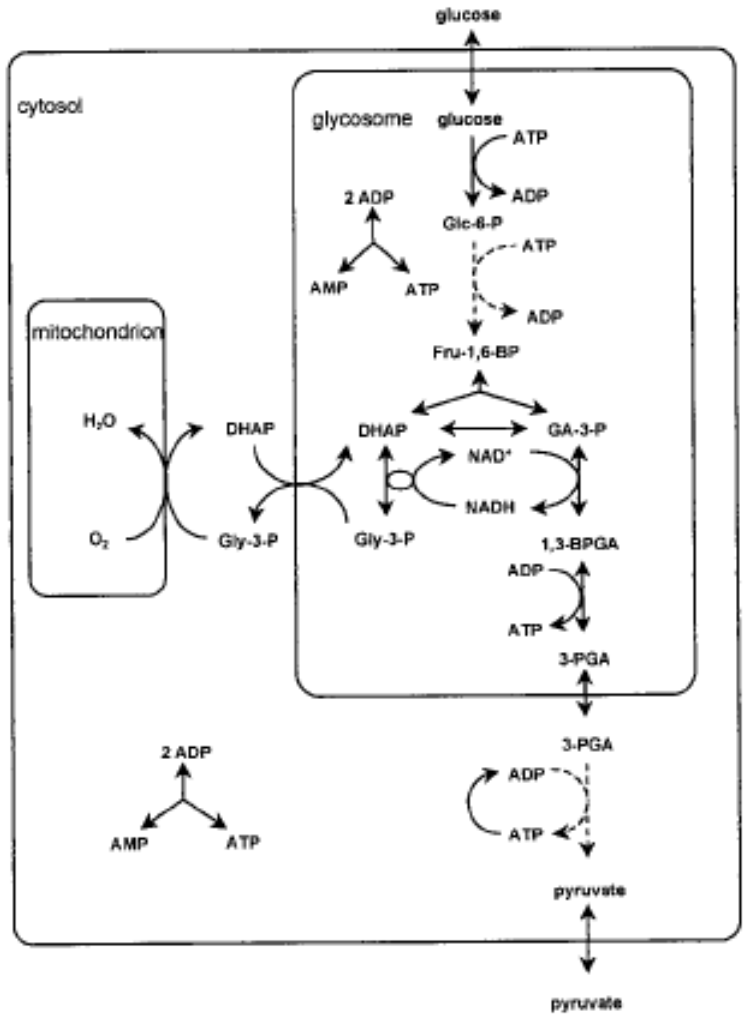

Fig. 1. A scheme of glycolysis in bloodstream-form *Trypanosoma brucei*. Solid lines represent reactions catalyzed by a single enzyme; dashed lines represent multiple sequential reactions. Glc-6-P, glucose 6-phosphate; Fru-1,6-BP, fructose 1,6-bisphosphate; GA-3-P, glyceraldehyde 3-phosphate; 1,3-BPGA, 1,3-bisphosphoglycerate; 3-PGA, 3-phosphoglycerate; DHAP, dihydroxyacetone phosphate; Gly-3-P, glycerol 3-phosphate.

$$\frac{d[\mathrm{Glc}]_{\mathrm{in}}}{dt} = \frac{v_{\text{glucose transport}} - v_{\mathrm{HK}}}{V_{\mathrm{tot}}} \quad [1]$$

$$\frac{d[\text{hexose-P}]}{dt} = \frac{v_{\mathrm{HK}} - v_{\mathrm{PFK}}}{V_{\mathrm{tot}}} \quad [2]$$

$$\frac{d[\text{Fru-1,6-BP}]}{dt} = \frac{v_{\mathrm{PFK}} - v_{\mathrm{ALD}}}{V_{\mathrm{tot}}} \quad [3]$$

$$\frac{d[\text{triose-P}]}{dt} = \frac{2v_{\mathrm{ALD}} - v_{\mathrm{GAPDH}} - v_{\mathrm{GDH}} + v_{\mathrm{GPO}}}{V_{\mathrm{tot}}} \quad [4]$$

$$\frac{d[\text{1,3-BPGA}]}{dt} = \frac{v_{\mathrm{GAPDH}} - v_{\mathrm{PGK}}}{V_{\mathrm{tot}}} \quad [5]$$

$$\frac{d[\mathrm{N}]}{dt} = \frac{v_{\mathrm{PGK}} - v_{\mathrm{PYK}}}{V_{\mathrm{tot}}} \quad [6]$$

$$\frac{d[\mathrm{pyruvate}]_{\mathrm{in}}}{dt} = \frac{v_{\mathrm{PYK}} - v_{\text{pyruvate transport}}}{V_{\mathrm{tot}}} \quad [7]$$

$$\frac{d[\mathrm{NADH}]}{dt} = \frac{v_{\mathrm{GAPDH}} - v_{\mathrm{GDH}}}{V_{\mathrm{tot}}} \quad [8]$$

$$\frac{d[\text{Gly-3-P}]}{dt} = \frac{v_{\mathrm{GDH}} - v_{\mathrm{GK}} - v_{\mathrm{GPO}}}{V_{\mathrm{tot}}} \quad [9]$$

$$\frac{d[\mathrm{P}]}{dt} = \frac{-v_{\mathrm{HK}} - v_{\mathrm{PFK}} + v_{\mathrm{PGK}} + v_{\mathrm{GK}} + v_{\mathrm{PYK}} - v_{\text{ATP utilization}}}{V_{\mathrm{tot}}} \quad [10]$$

in which:

$$[\text{hexose-P}] \equiv [\text{Glc-6-P}] + [\text{Fru-6-P}] \quad [11]$$

$$[\text{triose-P}] \equiv [\text{DHAP}] + [\text{GA-3-P}] \quad [12]$$

and

$$[\mathrm{N}] \equiv [\text{3-PGA}] + [\text{2-PGA}] + [\text{PEP}] \quad [13]$$

$$[\mathrm{P}] \equiv 2[\mathrm{ATP}] + [\mathrm{ADP}] \quad [14]$$

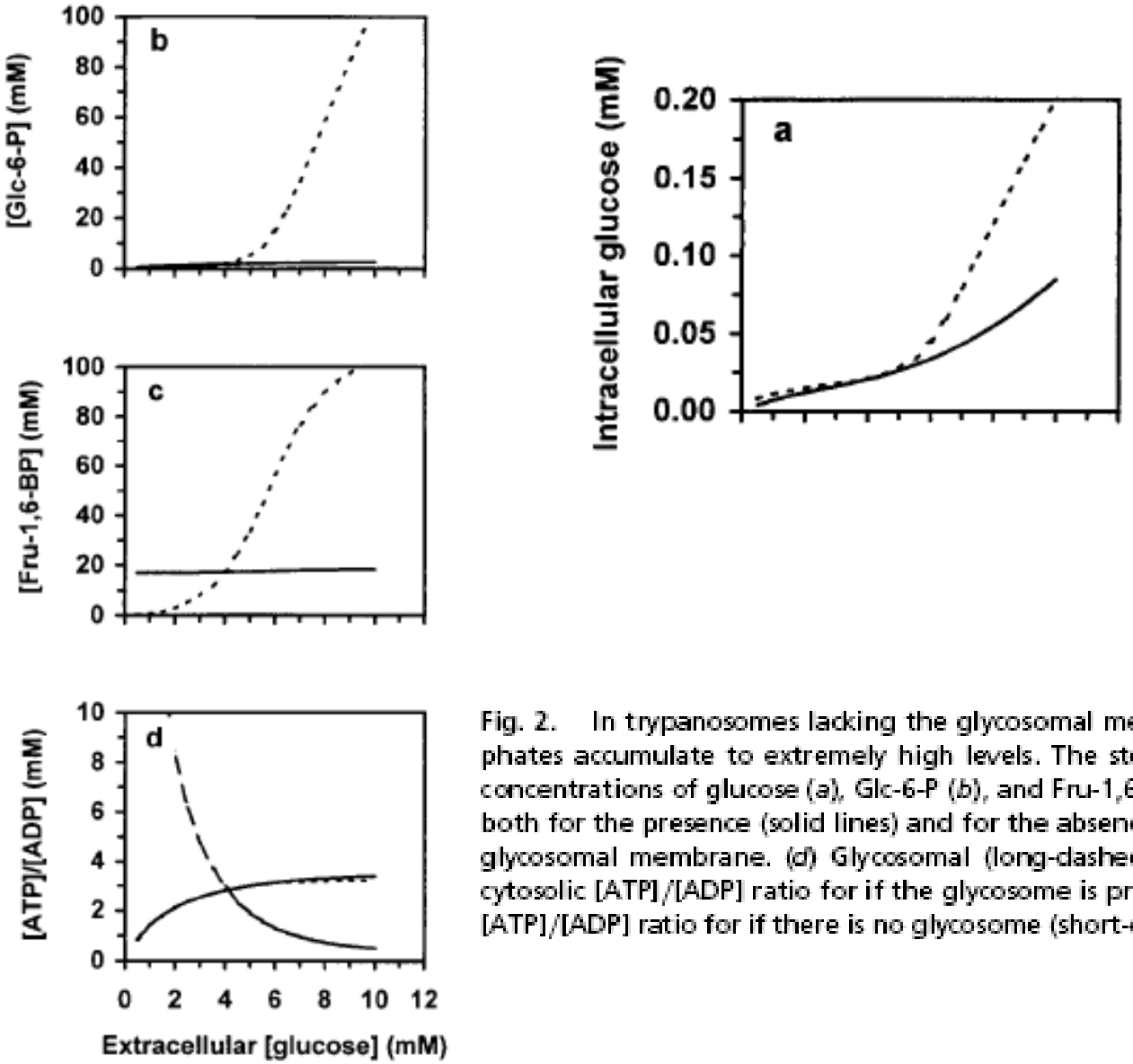

Fig. 2. In trypanosomes lacking the glycosomal membrane, hexose phosphates accumulate to extremely high levels. The steady-state intracellular concentrations of glucose (*a*), Glc-6-P (*b*), and Fru-1,6-BP (*c*) were calculated both for the presence (solid lines) and for the absence (dashed lines) of the glycosomal membrane. (*d*) Glycosomal (long-dashed line) and (solid line) cytosolic [ATP]/[ADP] ratio for if the glycosome is present and the cytosolic [ATP]/[ADP] ratio for if there is no glycosome (short-dashed line).

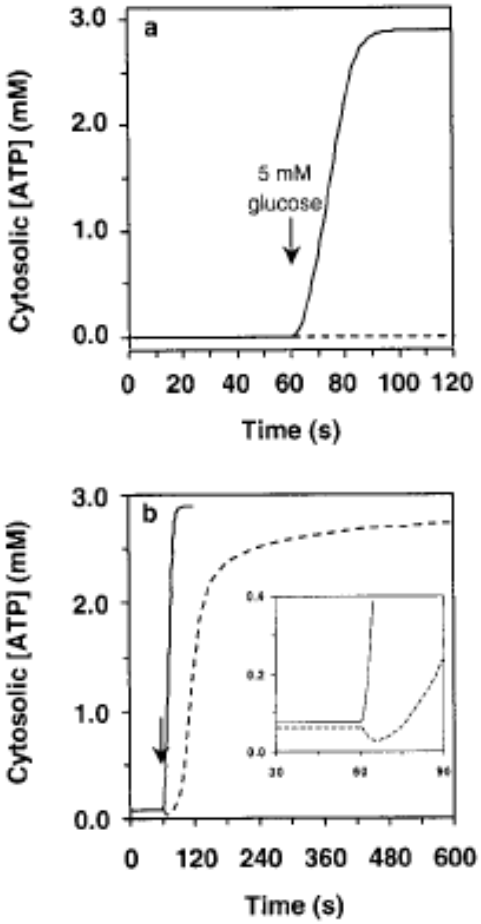

Fig. 3. The glycosome helps trypanosomes to recover from a low blood-glucose level when returning to a normal one. Trypanosomes consuming glucose in a steady state at 0.01 mM (*a*) or 0.05 mM (*b*) extracellular glucose, were given 5 mM glucose after 60 s. The cytosolic ATP concentration was monitored, both in the model with the glycosome (solid line) and in the model without the glycosome (dashed line). (*Inset*) Part from 30 to 90 s enlarged.

TABLE IV

The control of the glycolytic flux (C_i^J) and the displacement from equilibrium (Γ/K_{eq}) at increased glucose transport activity

Both the forward and the reverse V_{max} were increased by 35% so that the forward V_{max} became 143.4 nmol min^{-1} mg of $protein^{-1}$. The extracellular glucose concentration was 5 mM. All other parameters were the same as for Table I. Control coefficients above 5% are given in boldface.

Reaction	C_i^J	Γ/K_{eq}
	%	
Glucose transport	**8**	$6.0 \cdot 10^{-2}$
HK	5	$\ll 10^{-3}$
PFK	1	$\ll 10^{-3}$
ALD	**28**	0.15
GAPDH	**23**	0.21
PGK	**15**	$1.7 \cdot 10^{-3}$
PYK	1	$\ll 10^{-3}$
Pyruvate transport	0	$\ll 10^{-3}$
GDH	**17**	$9.6 \cdot 10^{-3}$
Glycerol-3-phosphate oxidase	2	$\ll 10^{-3}$
ATP utilization	0	

TABLE V

The inhibition of each individual enzyme required to inhibit the flux by 10 and 50%

These results were obtained at 5 mM glucose under aerobic conditions and at constant values of all other enzyme activities. The forward and reverse V_{max} were varied simultaneously by the same percentage.

Reaction	Inhibition required	
	10% flux reduction	50% flux reduction
	%	
Glucose transport	11	51
HK	77	93
PFK	87	93
ALD	44	76
GAPDH	53	84
PGK	61	85
PYK	94	97
GDH	56	83

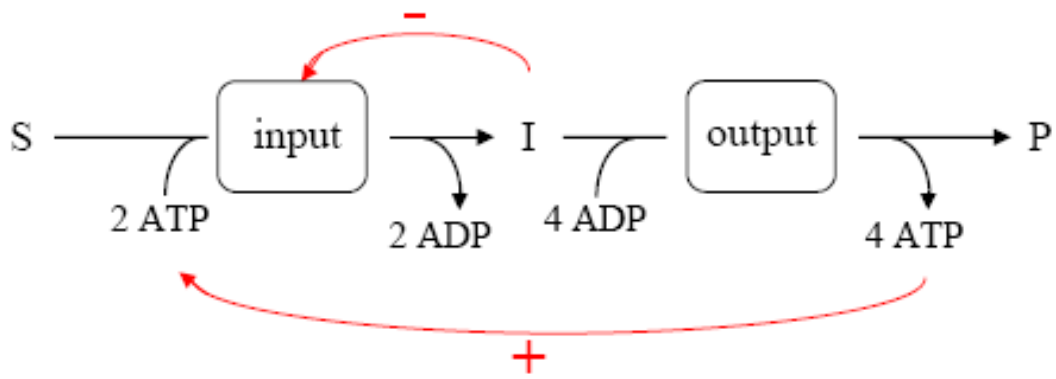
S
input
I
output
P
2 ATP
2 ADP
4 ADP
4 ATP
–
+

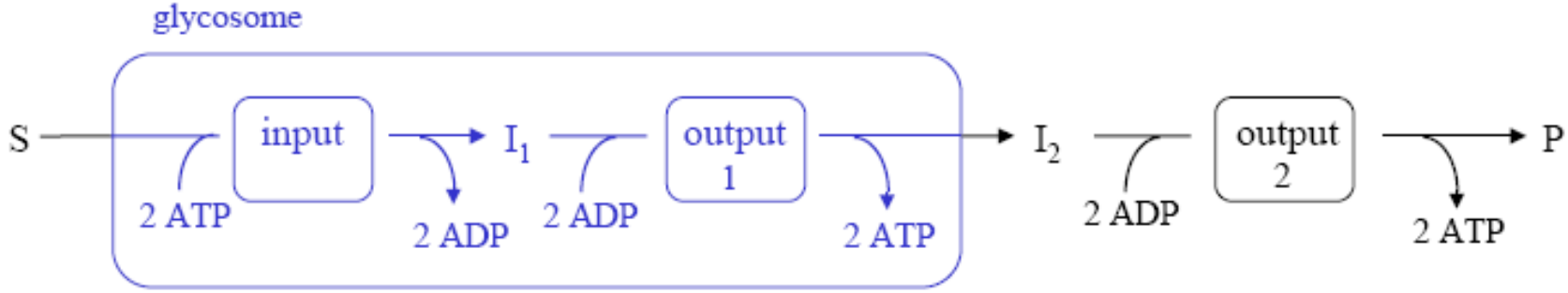
glycosome
S
input
I_1
output 1
I_2
output 2
P
2 ATP
2 ADP
2 ADP
2 ATP
2 ADP
2 ATP

INSECTO:
Glucosa: escasa
Lípidos: escasos
Aminoácidos: alta prolina y treoninal
Proteínas
Alta pO_2
Temperatura ambiente

SANGRE:
Glucosa: 50-120 mg por 100 ml
Lípidos (160-280 mg/dl FL, 120-125 mg/dl TG, 150-220 mg/dl colesterol)
Aminoácidos, 3-10 mg por 100 ml
Proteínas
pCO2: 40 mm Hg
pH 7.4
Temperatura cte.

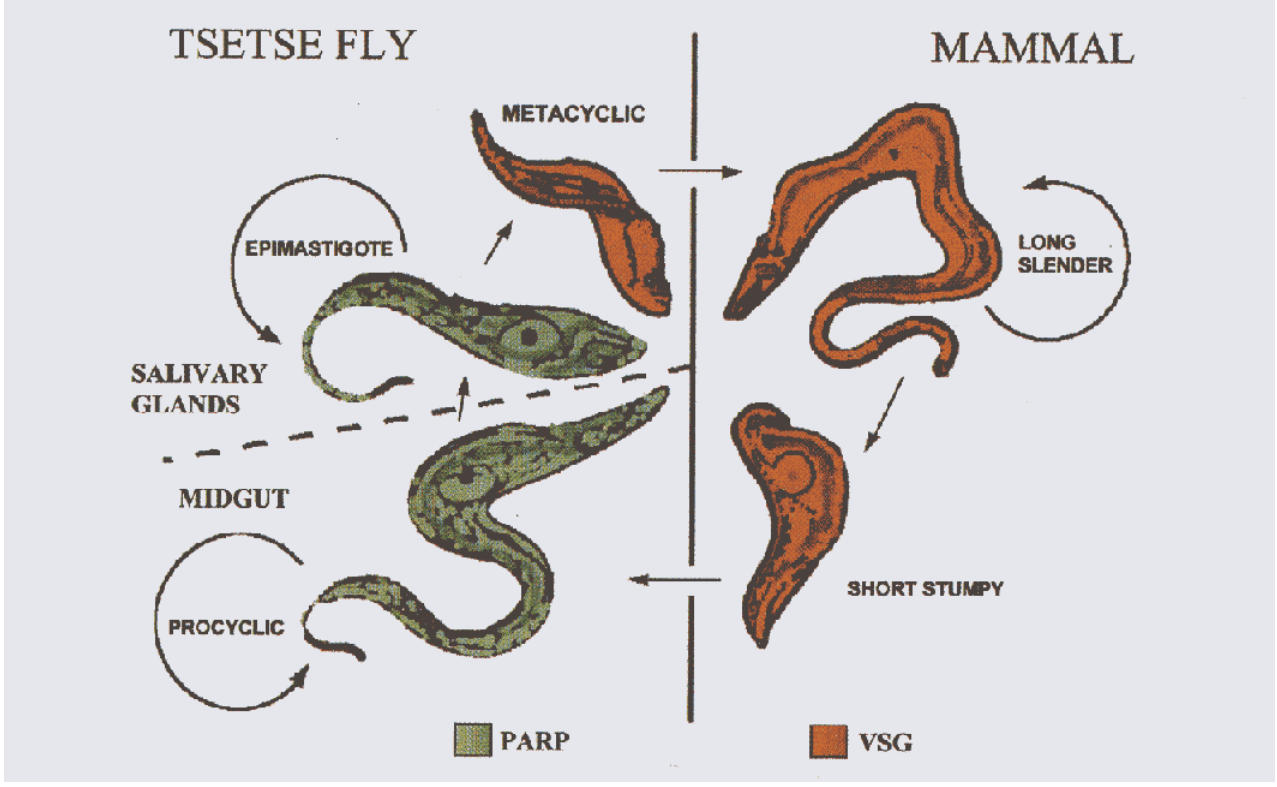

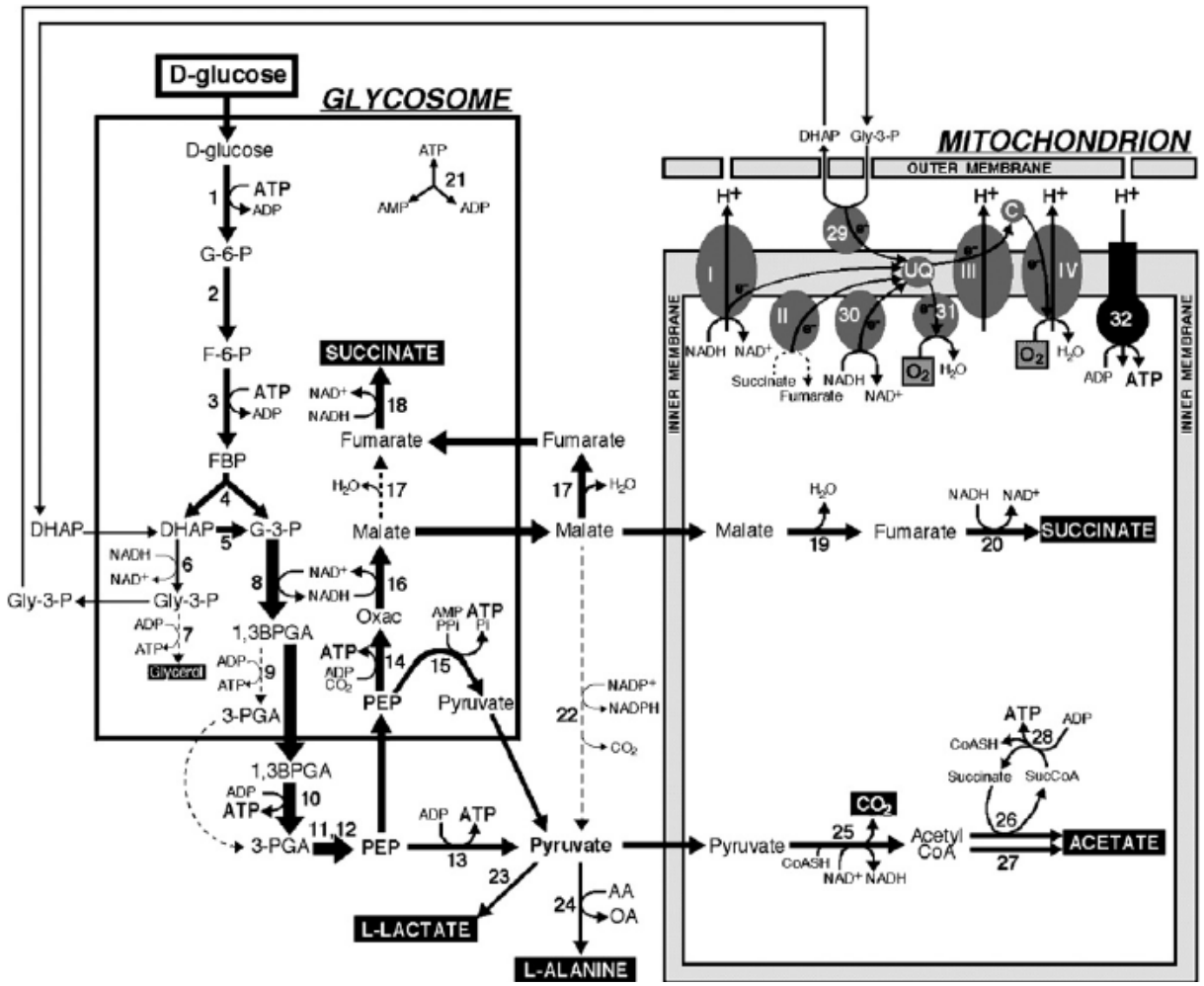

Fig. 2. Schematic representation of glucose metabolism in the procyclic form of *T. brucei*. Excreted end products of glucose metabolism (acetate, L-alanine, glycerol, L-lactate, succinate and CO_2) are in white characters on a black background. Arrows with different thicknesses tentatively represent the metabolic flux at each enzymatic step. Dashed arrows indicate steps which are supposed to occur at a background level or not at all. The mitochondrial outer membrane is permeable to metabolites and is only shown in the vicinity of the schematic electron-transport chain. Abbreviations: AA, amino acid; 1,3BPGA, 1,3-bisphosphoglycerate; C, cytochrome *c*; CoASH, coenzyme A; DHAP, dihydroxyacetone phosphate; F-6-P, fructose 6-phosphate; FBP, fructose 1,6-bisphosphate; G-3-P, glyceraldehyde 3-phosphate; G-6-P, glucose 6-phosphate; Gly-3-P, glycerol 3-phosphate; OA, 2-oxoacid; PEP, phospho*enol*pyruvate; 3-PGA, 3-phosphoglycerate; Pi, inorganic phosphate; PPi, inorganic pyrophosphate; SucCoA, succinyl-CoA; UQ, ubiquinone pool. Enzymes are: 1, hexokinase: 2, glucose-6-phosphate isomerase; 3, phosphofructokinase; 4, aldolase; 5, triosephosphate isomerase; 6, glycerol-3-phosphate dehydrogenase; 7, glycerol kinase; 8, glyceraldehyde-3-phosphate dehydrogenase; 9, glycosomal phosphoglycerate kinase; 10, cytosolic phosphoglycerate kinase; 11, phosphoglycerate mutase; 12, enolase; 13, pyruvate kinase; 14, phospho*enol*pyruvate carboxykinase; 15, pyruvate phosphate dikinase; 16, glycosomal malate dehydrogenase; 17, cytosolic (and glycosomal) fumarase (FHc); 18, glycosomal NADH-dependent fumarate reductase; 19, mitochondrial fumarase (FHm); 20, mitochondrial NADH-dependent fumarate reductase; 21, glycosomal adenylate kinase; 22, malic enzyme; 23, unknown enzyme; 24, alanine aminotransferase; 25, pyruvate dehydrogenase complex; 26, acetate:succinate CoA-transferase; 27, unknown enzyme; 28, succinyl-CoA synthetase; 29, FAD-dependent glycerol-3-phosphate dehydrogenase; 30, rotenone-insensitive NADH dehydrogenase; 31, alternative oxidase; 32, F_0F_1-ATP synthase; I, II, III and IV, complexes of the respiratory chain.

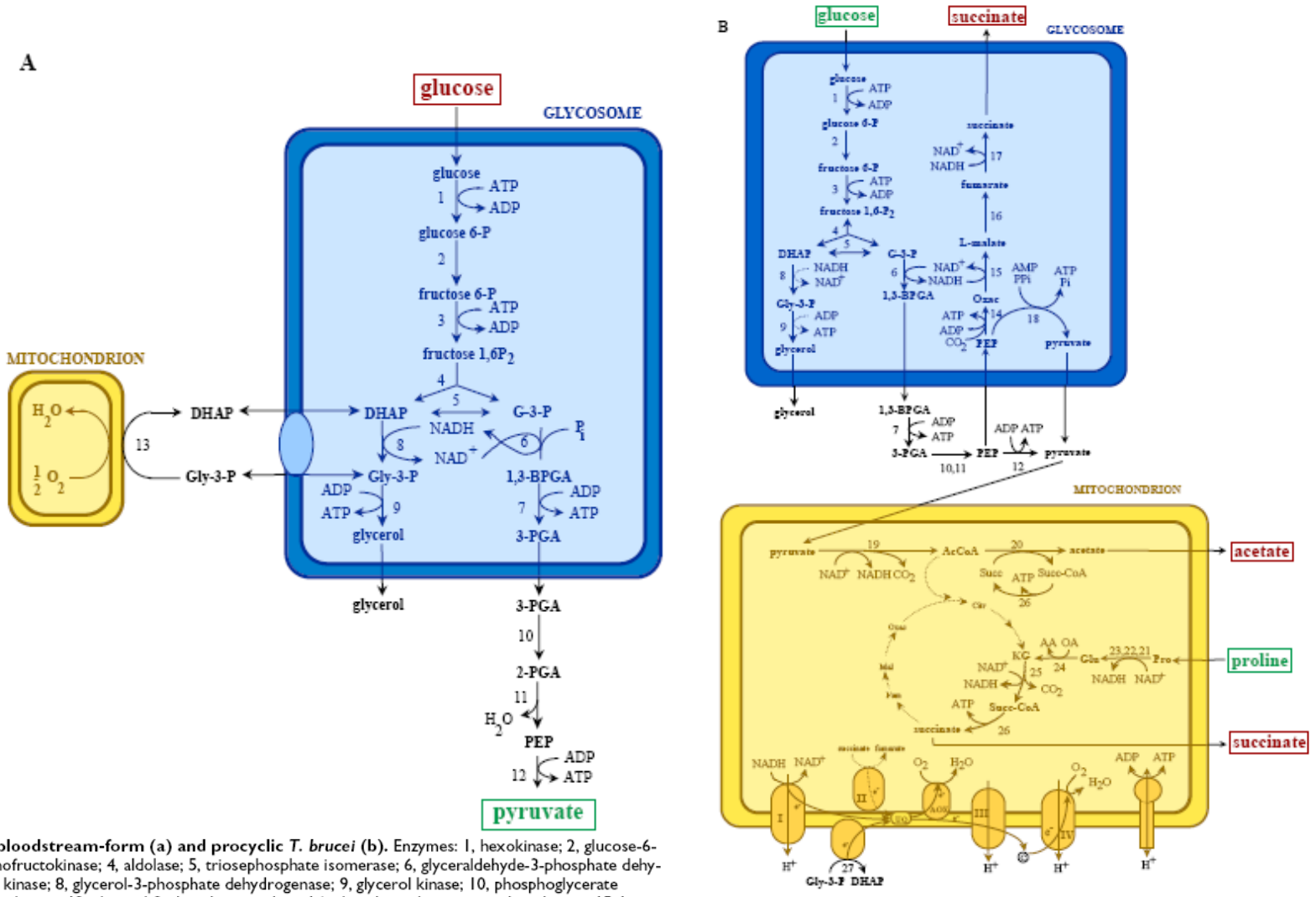

The energy metabolism of bloodstream-form (a) and procyclic *T. brucei* (b). Enzymes: 1, hexokinase; 2, glucose-6-phosphate isomerase; 3, phosphofructokinase; 4, aldolase; 5, triosephosphate isomerase; 6, glyceraldehyde-3-phosphate dehydrogenase; 7, phosphoglycerate kinase; 8, glycerol-3-phosphate dehydrogenase; 9, glycerol kinase; 10, phosphoglycerate mutase; 11, enolase; 12, pyruvate kinase; 13, glycerol-3-phosphate oxidase; 14, phospho*enol*pyruvate carboxykinase; 15, L-malate dehydrogenase; 16, fumarase; 17, fumarate reductase; 18, pyruvate phosphate dikinase; 19, pyruvate dehydrogenase complex; 20, acetate:succinate CoA transferase; 21, proline oxidase; 22, Δ'-pyrroline-5-carboxylate reductase; 23, glutamate semialdehyde dehydrogenase; 24, glutamate dehydrogenase; 25, α-ketoglutarate dehydrogenase; 26, succinyl CoA synthetase; 27, FAD-dependent glycerol-3-phosphate dehydrogenase. Abbreviations: AA, amino acid; AcCoA, acetyl-CoA; 1,3-BPGA, 1,3-bisphosphoglycerate; c, cytochrome c; Citr, citrate; DHAP, dihydroxyacetone phosphate; Fum, fumarate; G-3-P, glyceraldehyde 3-phosphate; Glu, glutamate; Gly-3-P, glycerol 3-phosphate; KG, α-ketoglutarate; Mal, malate; OA, 2-oxoacid; Oxac, oxaloacetate; PEP, phospho*enol*pyruvate; 3-PGA, 3-phosphoglycerate; Succ, succinate; Succ-CoA, succinyl-CoA; UQ, ubiquinone. Substrates and secreted end-products are indicated in green and red, respectively, and boxed. Enzymes involved in reactions represented by dashed lines are present, but experiments indicated that no significant fluxes occurred through these steps [62,95]. A complex II is depicted because succinate dehydrogenase activity and succinate-dependent repiration have been demonstrated in mitochondria of *T. brucei* procyclics and *T. cruzi* epimastigotes [167,168]. However the role of succinate respiration in the overall metabolism of these cells remains to be clarified. No evidence has been reported that electron transfer through complex I of the respiratory chain of trypanosomatids is coupled to proton expulsion. The mitochondrion contains two membranes; the inner membrane containing the respiratory chain and H^+-ATPase has been drawn in this figure.

Entamoeba

Giardia

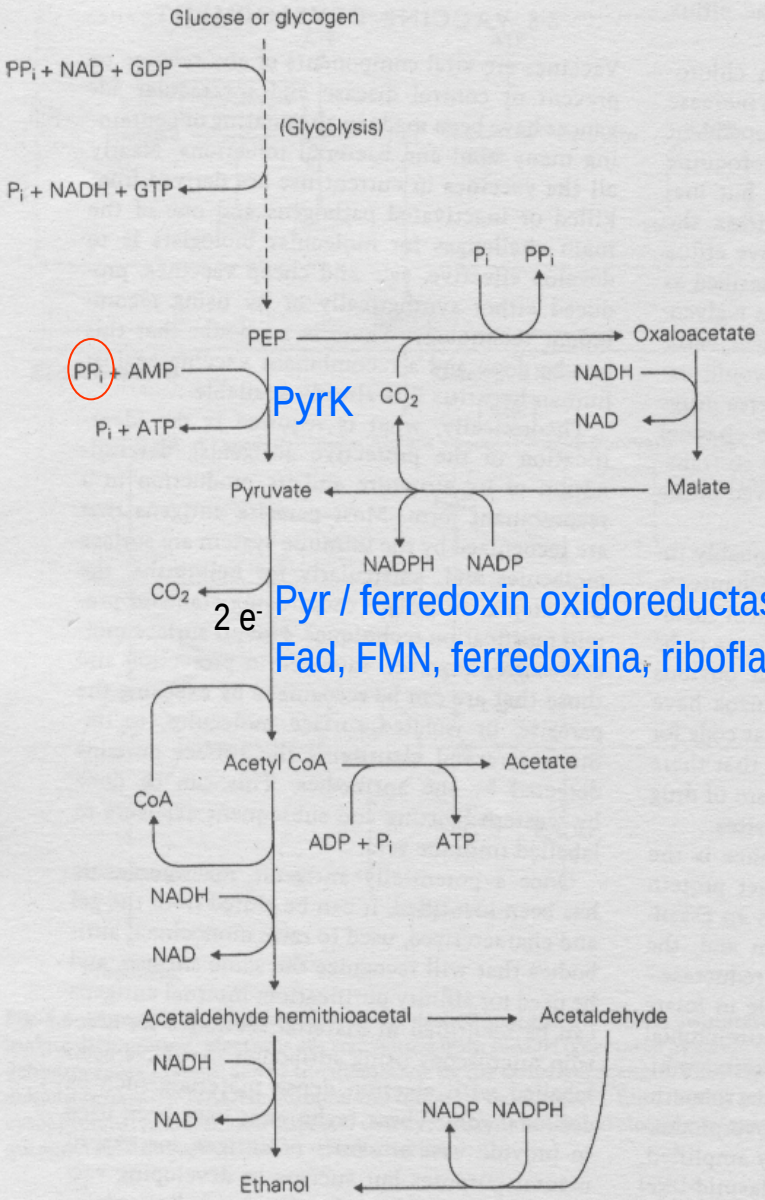

Fig. 5.3 Pathways of anaerobic glucose metabolism in *Entamoeba*. Those in *Giardia* are very similar but less completely known. P_i, PP_i – inorganic phosphate and pyrophosphate.

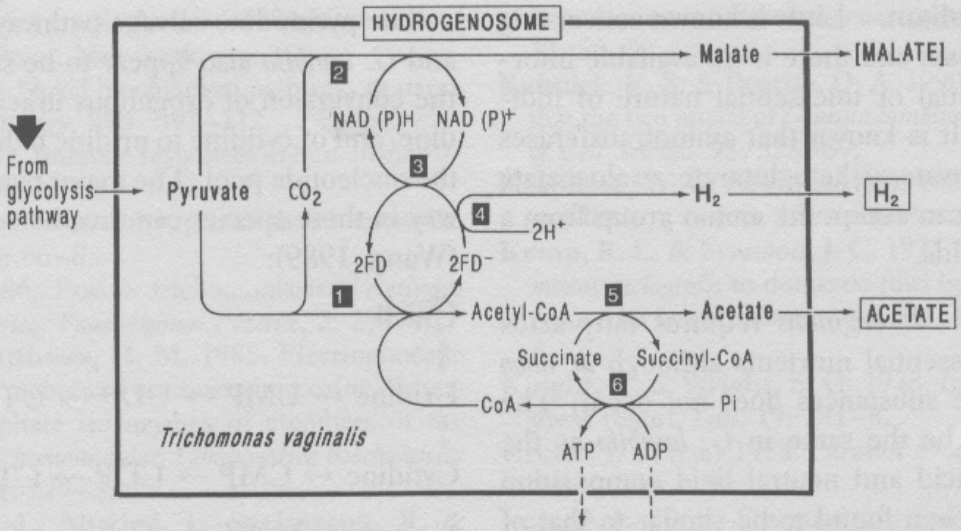

Fig. 4.9
Map of metabolism within the hydrogenosomes of *Trichomonas vaginalis* and *Tritrichomonas foetus*. [1] Pyruvate ferrodoxin oxidoreductase, [2] malate dehydrogenase (decarboxylating, NAD), [3] NAD : ferredoxin oxidoreductase, [4] H_2 : ferredoxin oxidoreductase, [5] acetate : succinate CoA-transferase, [6] succinate thiokinase. Hydrogen and acetate are the major end products and malate a minor one; see also Table 3.5. (Modified from Steinbüchel & Müller, 1986.)

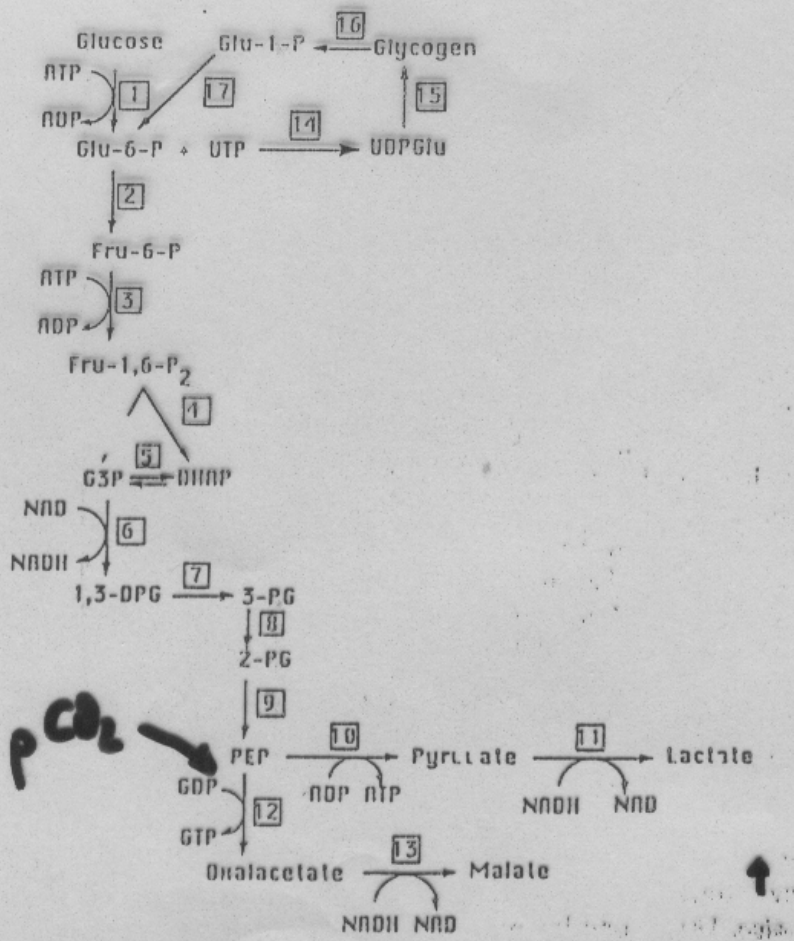

FIG. 4.1 Glycogenolysis and glycolysis in parasitic helminths. (1) hexokinase; (2) glucosephosphate isomerase; (3) phosphofructokinase; (4) aldolase; (5) triosephosphate isomerase; (6) glyceraldehyde-3-P dehydrogenase; (7) phosphoglycerate kinase; (8) phosphoglyceromutase; (9) enolase; (10) pyruvate kinase; (11) lactate dehydrogenase; (12) phosphoenolpyruvate carboxykinase; (13) malate dehydrogenase; (14) UDP glucosyl transferase; (15) glycogen synthase; (16) glycogen phosphorylase; (17) phosphoglucomutase.

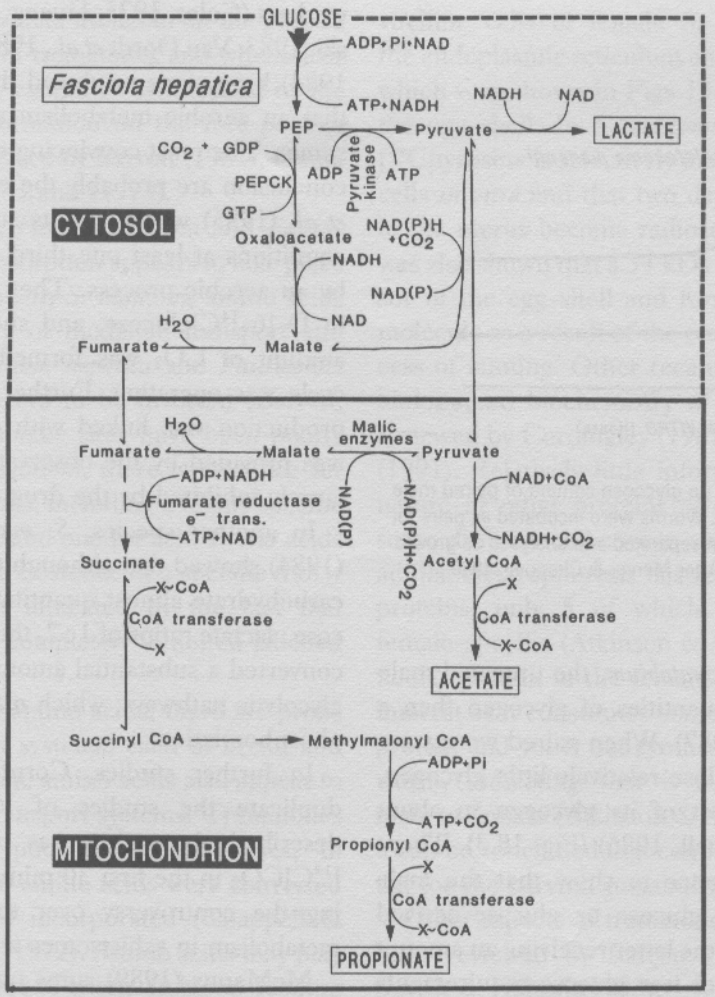

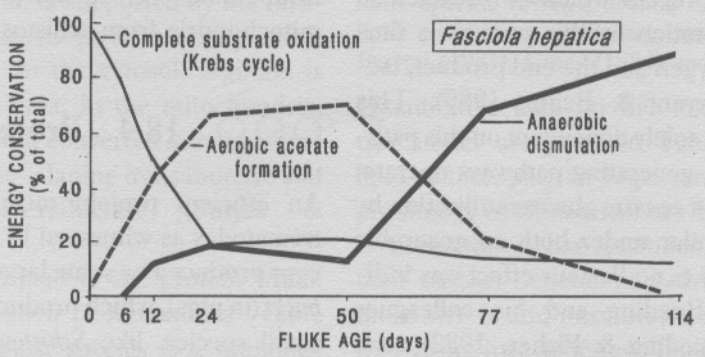

Fig. 18.1
Anaerobic energy metabolism in the adult liver fluke, *Fasciola hepatica*. Note that during the early phase of development, the metabolism is predominantly aerobic and a Krebs cycle operates; see Fig. 18.2. (Modified from Prichard, 1989.)

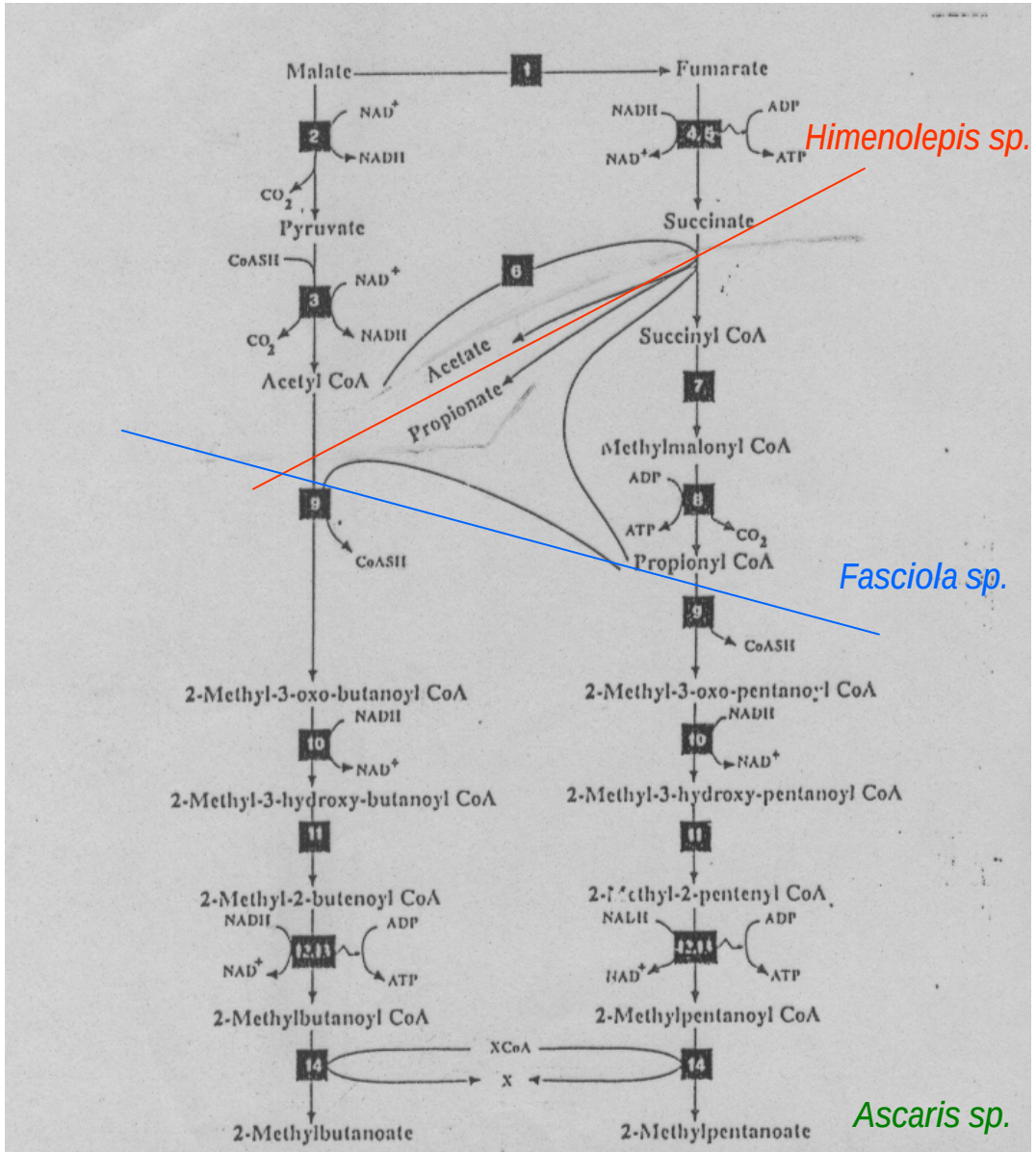

FIG. 4.2 Malate metabolism in mitochondria from body wall muscle of adult *Ascaris suum*. (1) Fumarase; (2) 'malic' enzyme; (3) pyruvate dehydrogenase complex; (4) complex I; (5) succinate-coenzyme Q reductase (complex II, fumarate reductase); (6) acyl CoA transferase; (7) methylmalonyl CoA mutase; (8) methylmalonyl CoA decarboxylase; (9) propionyl CoA condensing enzyme; (10) 2-methyl acetoacety CoA reductase; (11) 2-methyl-3-oxo-acyl CoA hydratase; (12) electron-transfer flavoprotein; (13) 2-methyl branched-chain enoyl CoA reductase; (14) acyl CoA transferase.

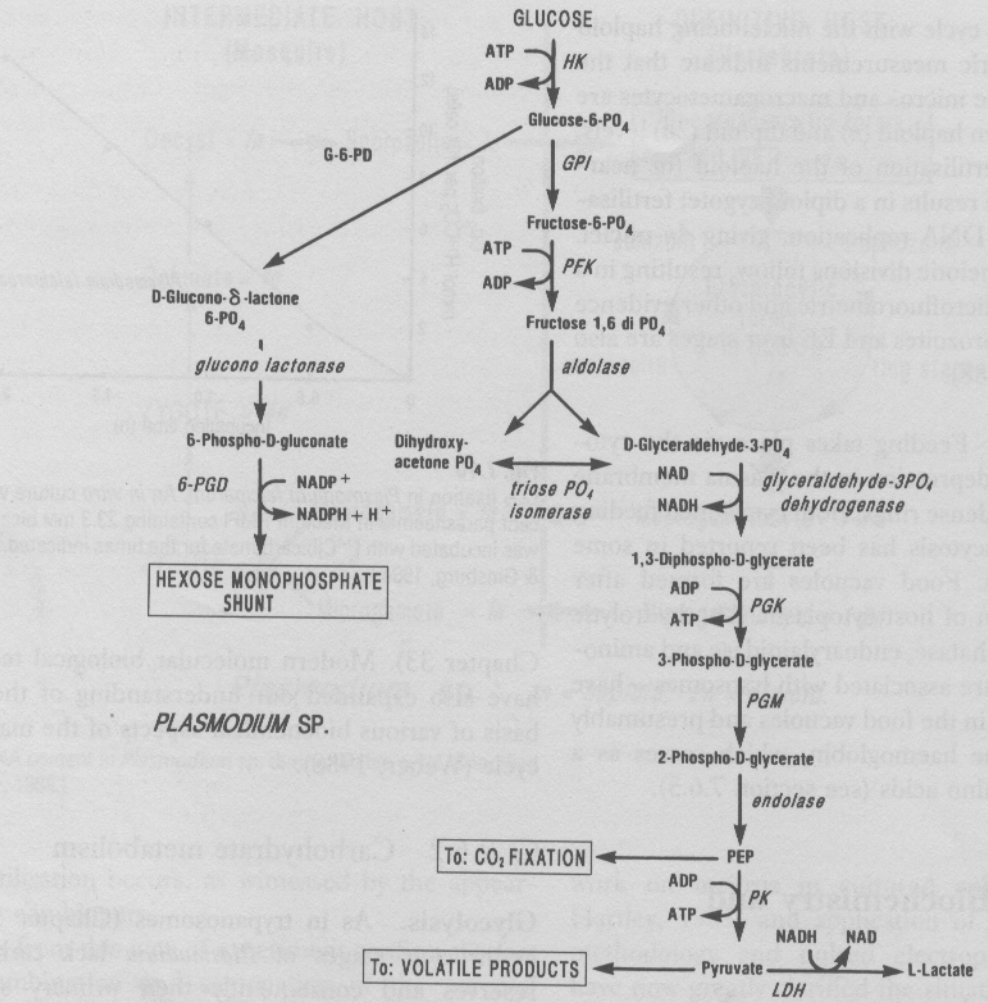

Fig. 7.11
Pathways of the glycolytic conversion of glucose in *Plasmodium* spp. Abbreviations (in italics) for enzymes, as follows: **HK**, hexokinase; **GPI**, glucose phosphate isomerase; **PFK**, phosphofructokinase; **PK**, pyruvate kinase; **LDH**, lactate dehydrogenase; **6-PGD**, 6-phosphogluconate dehydrogenase; **PGK**, phosphoglycerate kinase; **PGM**, phosphoglyceromutase. (Modified from Scheibel, 1988; reproduced with permission from *Malaria. Principles and Practice of Malariology* (ed. W. H. Wernsdorfer & I. McGregor), vol. 1, p. 182. Churchill-Livingstone, Edinburgh and London, 1988.)

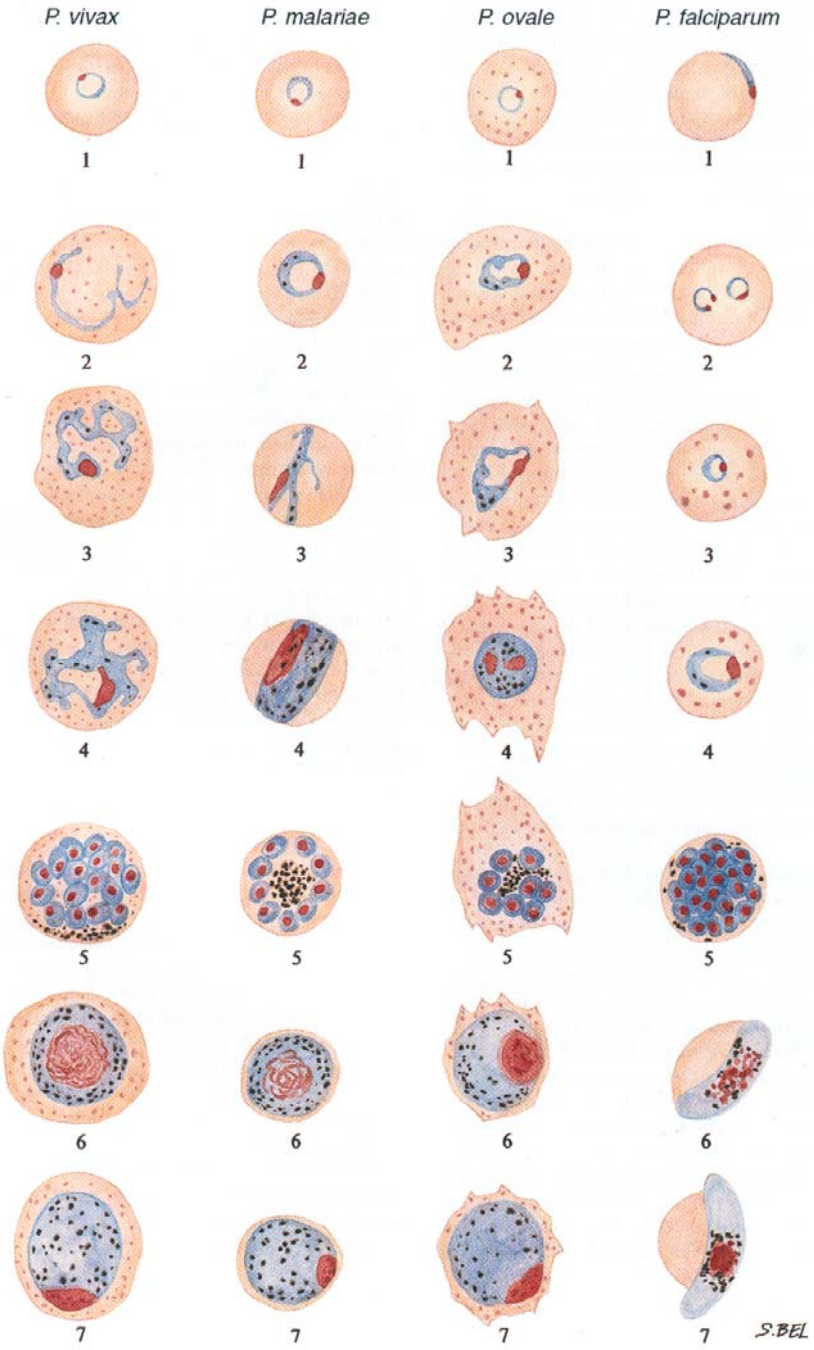

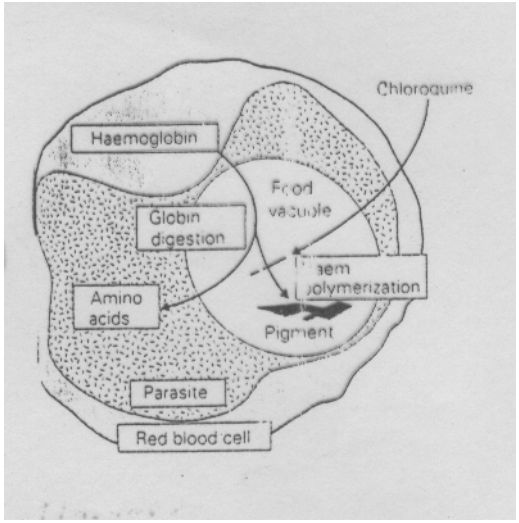

REACCION DE FENTON:

$$O_2^- + M^{n+1} \rightarrow M^n + O_2$$

$$\underline{M^n + H_2O_2 \rightarrow M^{n+1} + HO^- + HO^{\bullet}}$$

$$O_2^- + H_2O_2 \rightarrow HO^- + HO^{\bullet} + O_2$$

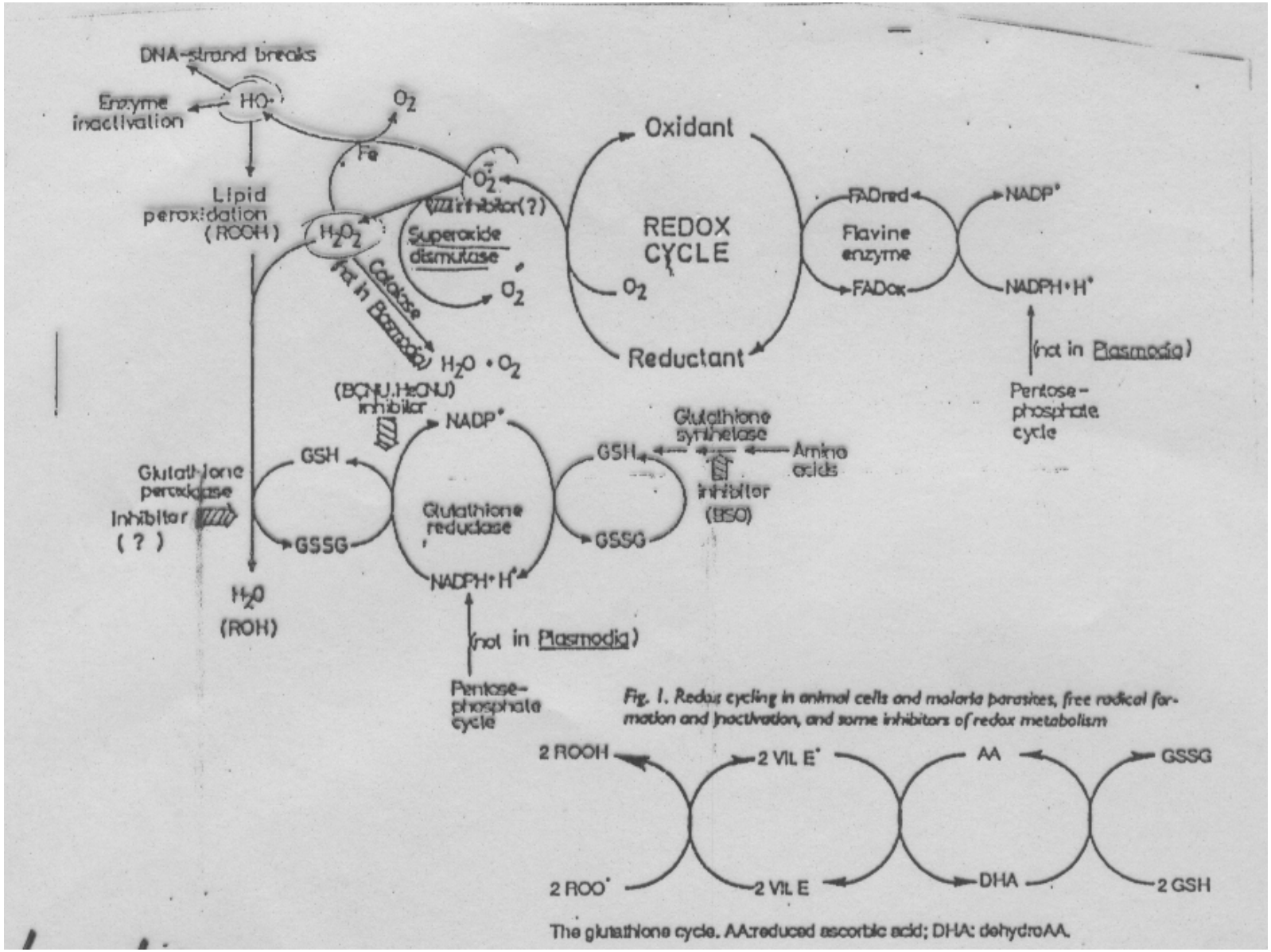

Fig. 1. Redox cycling in animal cells and malaria parasites, free radical formation and inactivation, and some inhibitors of redox metabolism

The glutathione cycle. AA:reduced ascorbic acid; DHA: dehydroAA.

Table 7.19 Host genetic factors in resistance to malaria[a]

Factor[b]	Comments
Hemoglobin disorders	
Sickling disorders	Includes sickle cell disease (SS), heterozygous states for sickle cell gene and those for hemoglobin C (SC) or β-thalassemia (S-thal); carrier state for sickle cell gene is AS; widely distributed throughout tropical Africa, parts of the Mediterranean, the Middle East, and central India; hemoglobin S confers protection against *P. falciparum* malaria (the parasite cannot complete life cycle due to cell sickling and destruction; reduced oxygen levels result in diminished parasite growth; reduced rosetting of RBCs in sickle carriers; protection also related to hemoglobin structure and parasite inability to metabolize)
Hemoglobins C and E	Data relating to selective advantage against malaria less convincing than for hemoglobin S; reduced parasite invasion and impaired growth have been documented; data for hemoglobin E have shown inconsistent results
Hemoblobin F	Growth of *P. falciparum* reduced in presence of hemoglobin F, thought to be due to hemoglobin itself rather than RBC properties; higher levels of hemoglobin F during first year of life might offer protection (newborn infants and adults with persistent fetal hemoglobin production)
Thalassemia (α and β)	Distribution of β-thalassemia coincides with that of malaria; 70% reduction in clinical malaria and 50% reduction in risk; although not seen in all geographic areas, in Papua New Guinea high protective effect of homozygous state for α-thalassemia against complications of *P. falciparum* malaria; babies under 2 yr (homozygous for α^+-thalassemia) had higher frequency of both *P. vivax* and *P. falciparum* but were resistant from 2 yr of age
Erythrocyte polymorphisms	
Glucose-6-phosphate dehydrogenase deficiency	Both female heterozygotes and male hemizygotes have reduced risk (around 50%) of developing severe malaria
Duffy-negative RBCs	Resistant to invasion by *P. vivax*
Ovalocytosis	Patients subject to severe malarial infection with high parasitemias; however, there is strong protection against cerebral malaria; structural change in RBC membrane interferes with binding of infected RBCs to vascular endothelium
Immunogenetic variants	
HLA genes	Each protective HLA type associated with 40–50% decrease in risk; these HLA types are common
HLA class I	HLA-A, -B, -C determine specificities of $CD8^+$ T cells (cytotoxic, major role in defense against intracellular pathogens); HLA-B35 frequency reduced in children with cerebral malaria and those with severe malarial anemia
HLA class II	HLA-DR, -DQ, -DP determine specificities of $CD4^+$ T cells that secrete cytokines and provide T-cell help for antibody production and action of other T cells; HLA-DRB1*1302–HLA-DQB1*1501 frequency reduced in children with severe malarial anemia
Cytokine, other immune response genes	
TNF	Major mediator of malaria fever; TNF is increased in children with cerebral malaria and markedly so in children with fatal cerebral malaria
MBL	Deficiency may be associated with increased susceptibility to infectious diseases; effect on malaria may be small to none
CD35	Also called complement receptor 1 (CR1); plays a role in rosetting; African variant of CR1 may protect against severe malaria

[a] Adapted from references 73 and 194.
[b] HLA, human leukocyte antigen; TNF, tumor necrosis factor; MBL, mannose-binding lectin.

Haplotype Diversity and Linkage Disequilibrium at Human *G6PD*: Recent Origin of Alleles That Confer Malarial Resistance

Sarah A. Tishkoff,[1,2*] Robert Varkonyi,[2] Nelie Cahinhinan,[2] Salem Abbes,[3] George Argyropoulos,[4] Giovanni Destro-Bisol,[5] Anthi Drousiotou,[6] Bruce Dangerfield,[7] Gerard Lefranc,[8] Jacques Loiselet,[9] Anna Piro,[10] Mark Stoneking,[11] Antonio Tagarelli,[10] Giuseppe Tagarelli,[10] Elias H. Touma,[9] Scott M. Williams,[12†] Andrew G. Clark[2]

The frequencies of low-activity alleles of glucose-6-phosphate dehydrogenase in humans are highly correlated with the prevalence of malaria. These "deficiency" alleles are thought to provide reduced risk from infection by the *Plasmodium* parasite and are maintained at high frequency despite the hemopathologies that they cause. Haplotype analysis of "A−" and "Med" mutations at this locus indicates that they have evolved independently and have increased in frequency at a rate that is too rapid to be explained by random genetic drift. Statistical modeling indicates that the A− allele arose within the past 3840 to 11,760 years and the Med allele arose within the past 1600 to 6640 years. These results support the hypothesis that malaria has had a major impact on humans only since the introduction of agriculture within the past 10,000 years and provide a striking example of the signature of selection on the human genome.

Early Origin and Recent Expansion of *Plasmodium falciparum*

Deirdre A. Joy,[1*] Xiaorong Feng,[1] Jianbing Mu,[1] Tetsuya Furuya,[1] Kesinee Chotivanich,[2] Antoniana U. Krettli,[3] May Ho,[4] Alex Wang,[5] Nicholas J. White,[2] Edward Suh,[5] Peter Beerli,[6] Xin-zhuan Su[1]

The emergence of virulent *Plasmodium falciparum* in Africa within the past 6000 years as a result of a cascade of changes in human behavior and mosquito transmission has recently been hypothesized. Here, we provide genetic evidence for a sudden increase in the African malaria parasite population about 10,000 years ago, followed by migration to other regions on the basis of variation in 100 worldwide mitochondrial DNA sequences. However, both the world and some regional populations appear to be older (50,000 to 100,000 years old), suggesting an earlier wave of migration out of Africa, perhaps during the Pleistocene migration of human beings.